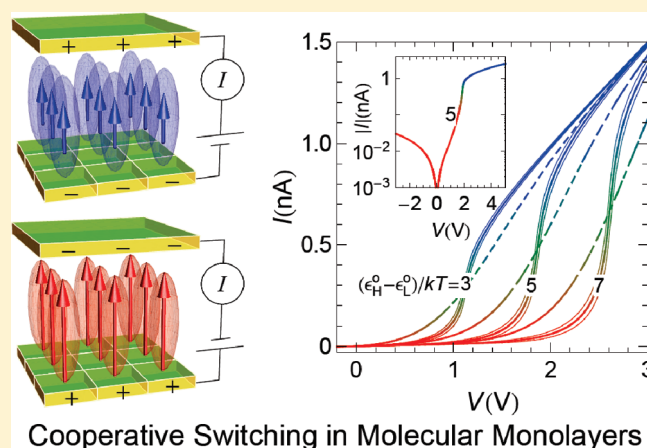


# Cooperative Effects Enhance Electric-Field-Induced Conductance Switching in Molecular Monolayers

José A. Manzanares, Javier Cervera, and Salvador Mafé\*

Department de Termodinàmica, Facultat de Física, Universitat de València, E-46100 Burjassot, Spain

**ABSTRACT:** The anchoring of molecules with functional groups at surfaces permits information processing based on two stable molecular states that can be tuned externally by light irradiation and external fields. By using a molecular model that incorporates the essential characteristics of the problem, we show that the local interactions between adjacent molecules in a densely packed monolayer can stabilize domains with the same molecular state because of cooperative processes, enhancing significantly the switching properties between the molecular states. The case of electric-field-induced conductance switching is exploited in two possible applications: the design of a logic gates system and the operation of a sensing layer based on the modulation of the monolayer conductance by a ligand from an external solution. Extensions to other experimental systems (electrical and optical switches based on nanoparticles with ligand shells, molecular dipoles, and nanomagnets) where collective effects should be present can also be considered on the basis of the proposed concepts.



Cooperative Switching in Molecular Monolayers

## INTRODUCTION

Switching and sensing in molecular monolayers are central to biology and nanoelectronics. The anchoring of molecules with functional groups at surfaces allows implementing information processing based on two stable molecular states that can be tuned by light irradiation and external fields.<sup>1–7</sup> Applications concerning data storage devices, sensors, and molecular machines require significant changes of a measurable property in response to an input stimulus. Because molecules show weak electrical and optical signals, experimental methods to enhance the system response are needed. An obvious choice is to exploit the collective effects characteristic of densely packed molecules.<sup>2,8</sup> The local interactions between adjacent molecules may stabilize domains with the same state, enhancing switching and sensing because of cooperative processes. We explore theoretically the essential characteristics needed to exploit cooperativity in monolayers with a finite number of molecules. Electric field-induced conductance switching<sup>3–6</sup> is analyzed, but extensions to other experimental systems (e.g., optical switches<sup>1,2,8</sup>) should also be possible using similar concepts. Since digital information processing requires switching between two high (H) and low (L) conductive states separated by a narrow transition region, our results may assist in the development of nanostructures with collectively enhanced switching properties.

High-resolution theoretical methods have been considered to describe particular molecules and surfaces,<sup>3,9,10</sup> but phenomenological models emphasizing the collective effects useful for practical applications are lacking. These models should compare the characteristic energies of the molecule–surface, molecule–molecule,

and molecule–external field interactions with the thermal energy  $kT$  (where  $k$  is Boltzmann's constant and  $T$  is the temperature) because it is the balance between these terms that determines the monolayer response to the electric field  $E$ . In particular,  $E$  can trigger a  $L \rightleftharpoons H$  transition in the monolayer if the molecules have large electric dipole moments  $p$  or polarizabilities so that the change in dipolar energy  $(p_L - p_H)E$  may exceed the transition barrier energy  $(\epsilon_L - \epsilon_H)$  between two molecular states of low and high conductances.<sup>3–5</sup> In the absence of intermolecular interactions (isolated molecules in monolayers with low molecular density), the competition between the energies  $kT$ ,  $(p_L - p_H)E$ , and  $(\epsilon_L - \epsilon_H)$  dictates the switching between two monolayer conductance states.<sup>11</sup> Remarkably, in densely packed monolayers the local interactions between adjacent neighbors can stabilize a finite number (domain) of molecules predominantly in the same state over a few tens of nanometers, and this cooperative process enhances switching.<sup>2</sup> The collective behavior requires the introduction of additional interaction energies to describe the emerging cooperative phenomena.<sup>12</sup> We address this question here using fundamental concepts that should find application in molecular electronic switches based on nanoparticles with ligand shells,<sup>13</sup> molecular dipoles,<sup>12,14</sup> and immobilized molecules in self-assembled monolayers.<sup>1,2</sup>

The collective transition of a molecular domain involves local changes that can be induced by irradiation, heating, change in the

Received: March 9, 2011

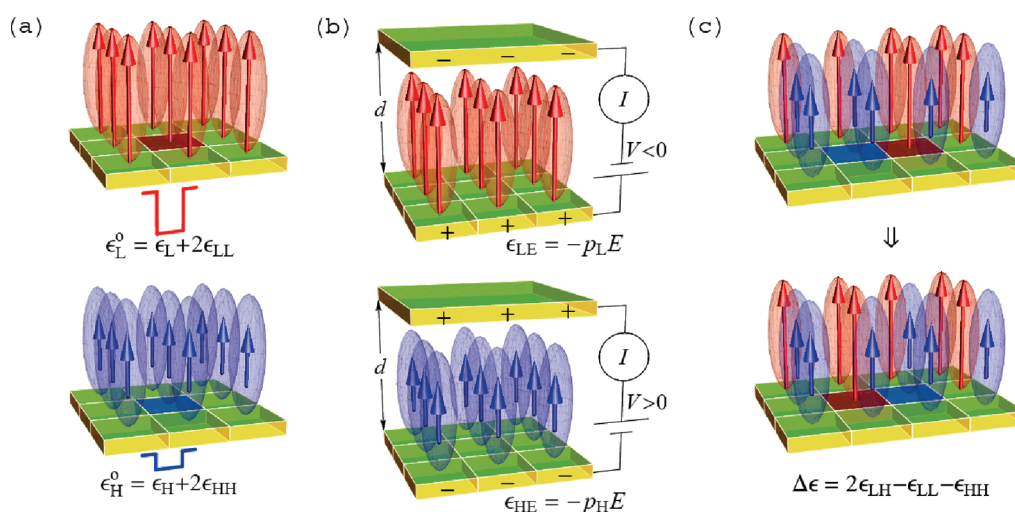


**Figure 1.** Schematic monolayer of molecules in two conformational states L and H with effective dipole moments  $p_L$  and  $p_H$  ( $p_L > p_H$ ) (a). The molecules can switch conformation because of the dipolar electrical energies  $\epsilon_{LE}$  and  $\epsilon_{HE}$  (b). When two neighboring molecules change their states as shown in (c) the energy change due to the local interactions is equal to the exchange energy  $\Delta\epsilon$ .

chemical environment, or external fields. Designing a switch based on a domain of the monolayer can eliminate the need for access to individual molecules. The control of single molecules and connection to the external environment is difficult, and in addition, nanoscale building blocks can show large variability in their individual properties.<sup>15</sup> On the contrary, small domains of molecules could still be used as reliable switches because of the averaging effect of many units interacting cooperatively.<sup>2</sup> Collective effects should be enhanced at the nanoscale because the state of a given molecule in a densely packed domain is influenced by the states of the nearest neighbors (cooperative electronic phenomena are characteristic of two-dimensional molecular arrangements, enabling detection of different physicochemical effects).<sup>16,17</sup>

Previous studies emphasizing collective phenomena have been focused on the stability and phase separation in multicomponent systems of mixed monolayers,<sup>18</sup> the effects of the electrical field and molecule polarizability on bistability,<sup>19</sup> and the case of mixed parallel and antiparallel dipole monolayers.<sup>17</sup> We describe the monolayer conductance switching using a phenomenological model for cooperativity without specificity to any particular molecular system. As possible applications that exploit the switching characteristics, we consider the cases of a logic gate and a sensing layer based on the modulation of the conductance by a ligand from an external solution. Although electric field-induced conductance switching is emphasized, extensions to other experimental systems (electrical and optical switches based on nanoparticles with ligand shells, molecular dipoles, and nanomagnets) where collective effects should be significant could also be considered on the basis of the proposed concepts.

## MODEL

Mechanisms proposed to explain the changes observed in the conductance of molecules include different electron tunneling rates due to the different molecule lengths in two states, changes in the electronic structure of the molecule–surface junction, and reversals in the relative orientation of the internal dipole field and the external field. Following previous phenomenological models,<sup>11,12</sup> we assume that the monolayer can show two macroscopic conductances  $g_L$  and  $g_H$  ( $g_L \ll g_H$ ) associated with two molecular states that differ in molecule–substrate, molecule–molecule, and

molecule–field interaction energies (Figures 1a–1c). The monolayer conductance is  $g_L$  ( $g_H$ ) when all the molecules are in the L (H) state. In general, however,  $g$  is intermediate between  $g_L$  and  $g_H$  and determined by the states of the individual molecules. Because these states can be tuned externally by means of an applied voltage, switching between  $g_L$  and  $g_H$  is possible.

We use the statistical thermodynamics formalism by Hill<sup>12,20</sup> and Ben-Naim,<sup>21</sup> who studied dipole cooperativity in biological membranes and macromolecules, to obtain the average numbers of molecules in each state as a function of the external conditions (temperature and voltage). The model is based on the following experimental facts:<sup>1,2,4–6,8,14,16,17,22</sup> (i) molecular monolayers that respond to changes in the external electric field and other environmental conditions are available; (ii) molecular engineering of the dipole moments by selecting the appropriate chemical groups and their subsequent assembly into approximately defined architectures has been demonstrated; (iii) local interactions between molecular dipoles are responsible for the observed cooperative phenomena; and (iv) promotion or suppression of electron transfer in dipole monolayers is due to changes in the locally high dipolar field. Theoretical studies have also shown significant dipole moment variation and tuning of the molecular conduction with the field.<sup>9,10,19,23</sup>

A molecular description is complicated because not only the electrical dipole–dipole and dipole–field interactions are important but also other effects such as the molecule–surface coupling,<sup>1–3,7</sup> field-induced elastic deformations,<sup>3–5,9</sup> polarizability phenomena,<sup>19</sup> and the spatial packing of the molecules<sup>1,2,5,14,17,18</sup> should be of relevance. (In particular, while neighboring dipoles may be oriented in a stable antiparallel pair state canceling out the total dipole, the dipole immobilization on surfaces and some particular packing structures can also stabilize the parallel orientation.<sup>14</sup>)

The model of Figure 1 incorporates the basic features needed for switching while keeping the complexity to a minimum. The monolayer is composed of  $N$  molecules on a lattice, and there are three contributions to the molecular energies. The molecule–surface interaction makes the molecular state L more stable than the H state (the difference in the adsorption energies  $\epsilon_H - \epsilon_L > 0$  can be considered as a transition energy barrier). Allowing for molecule–molecule interactions restricted to the  $c$  nearest neighbors,

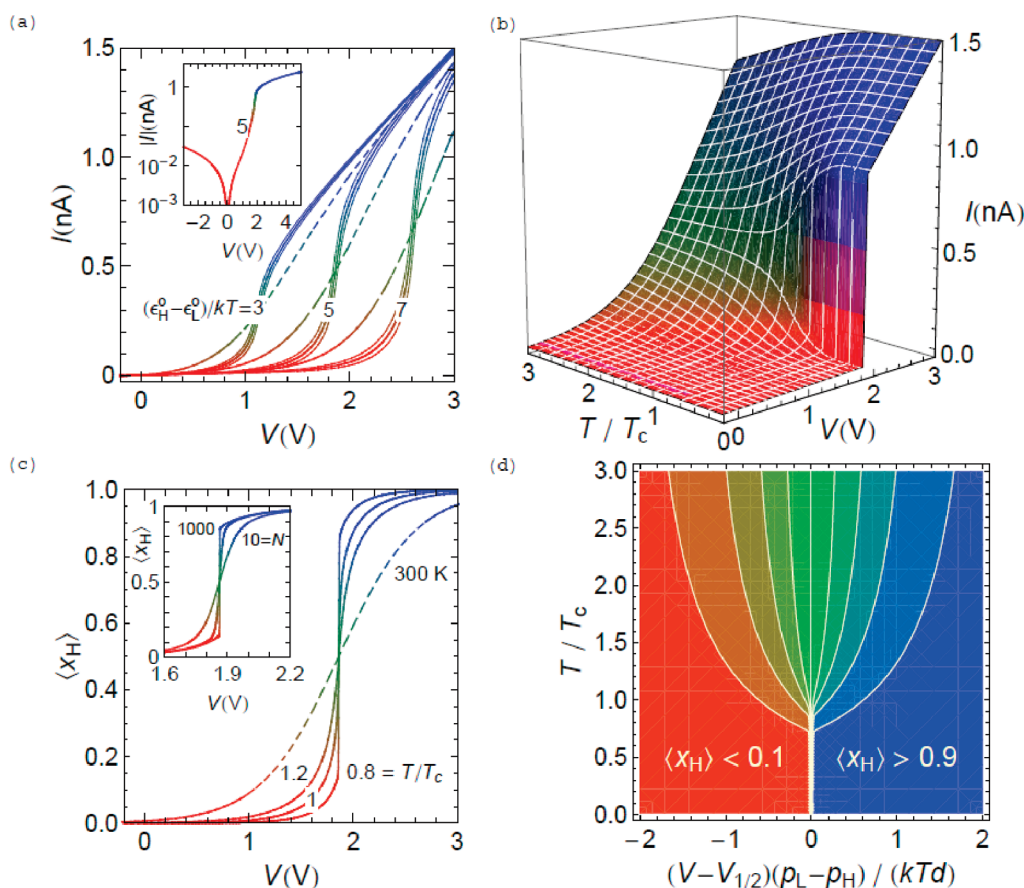


**Figure 2.** Monolayer  $I$ – $V$  curve and rectification characteristics (inset in logarithmic scale for  $(\epsilon_{\text{H}}^0 - \epsilon_{\text{L}}^0)/kT = 5$ ) at  $T = 300$  K and different values of  $(\epsilon_{\text{H}}^0 - \epsilon_{\text{L}}^0)/kT$  with  $g_{\text{L}} = 10$  pS. The noncooperative behavior ( $T_{\text{c}} = 0$ , dashed curves) is shown for comparison. The broadening of the curves, which is represented by the thin lines, is due to the thermal noise (a). The  $I$ – $V$  curve at different  $T/T_{\text{c}}$  for  $(\epsilon_{\text{H}}^0 - \epsilon_{\text{L}}^0)/k = 1500$  K (b).  $\langle x_{\text{H}} \rangle$  vs  $V$  for  $(\epsilon_{\text{H}}^0 - \epsilon_{\text{L}}^0)/k = 1500$  K at  $T/T_{\text{c}} = 0.8, 1.0$ , and  $1.2$ , and the noncooperative behavior (dashed line) at  $300$  K. The inset shows  $\langle x_{\text{H}} \rangle$  vs  $V$  for  $N = 10, 50$ , and  $1000$ ,  $T = 200$  K, and  $(\epsilon_{\text{H}}^0 - \epsilon_{\text{L}}^0)/k = 1500$  K (c). Contour plot of  $\langle x_{\text{H}} \rangle$  as a function of  $T/T_{\text{c}}$  and  $(V - V_{1/2})(p_{\text{L}} - p_{\text{H}})/(kTd) = \ln s$ . The contours shown are  $\langle x_{\text{H}} \rangle = 0.1, 0.2, \dots, 0.9$  (d). The curves have been colored according to the  $\langle x_{\text{H}} \rangle$  values as shown in (d) and calculated for  $N = 200$  (except for the inset in (c)).

where  $c$  is the coordination number of the lattice, the molecular energy in a “pure” monolayer in state L (H) is  $\epsilon_{\text{L}}^{\circ} \equiv \epsilon_{\text{L}} + c\epsilon_{\text{LL}}/2 < 0$  ( $\epsilon_{\text{H}}^{\circ} \equiv \epsilon_{\text{H}} + c\epsilon_{\text{HH}}/2 < 0$ ). Although the repulsive interactions between molecules in like states may render the effective energy barrier  $\epsilon_{\text{H}}^{\circ} - \epsilon_{\text{L}}^{\circ} > 0$  somewhat lower than  $\epsilon_{\text{H}} - \epsilon_{\text{L}} > 0$ , the molecular state L is stable in monolayers when no electric field is applied (Figure 1a). The molecules also switch conformation under the influence of an external field  $E = -V/d$ , where  $V$  is the applied voltage across the electrode separation  $d$  (Figure 1b). At low  $V$ , the molecular state L is still stable because of its low energy compared to state H. As the voltage  $V$  is increased, however, the molecule–field interaction energy promotes an electric field-driven molecular transition from state L to H. Note that the energy barrier  $(\epsilon_{\text{H}}^{\circ} - \epsilon_{\text{L}}^{\circ})$  and the difference in the dipole–field interaction energies  $(p_{\text{L}} - p_{\text{H}})E$  should be at least of the order of the thermal energy  $kT$  to avoid random changes in the molecular states caused by thermal fluctuations (stochastic switching should be avoided for the voltage-triggered switching to be efficient).<sup>24,25</sup> Finally, the monolayer can exhibit phase separation phenomena (i.e., formation of molecular domains) if the exchange energy  $\Delta\epsilon \equiv 2\epsilon_{\text{LH}} - \epsilon_{\text{LL}} - \epsilon_{\text{HH}}$  is positive (Figure 1c); contrarily, mixing of molecules in different states is promoted if the exchange energy is negative, and the monolayer shows then a single phase of uniform composition under equilibrium conditions.

In the presence of an electric field  $E$ , the monolayer energy is  $\epsilon(E) = \epsilon(0) - (N_{\text{L}}p_{\text{L}} + N_{\text{H}}p_{\text{H}})E$ , where  $\epsilon(0) = N_{\text{L}}\epsilon_{\text{L}} + N_{\text{H}}\epsilon_{\text{H}} + N_{\text{LL}}\epsilon_{\text{LL}} + N_{\text{HH}}\epsilon_{\text{HH}} + N_{\text{LH}}\epsilon_{\text{LH}} = N_{\text{L}}\epsilon_{\text{L}}^{\circ} + N_{\text{H}}\epsilon_{\text{H}}^{\circ} + (N_{\text{LH}}/2)\Delta\epsilon$  is the energy in the absence of field;  $\epsilon_i < 0$  is the molecule–surface interaction energy;  $\epsilon_{ij}$  is the molecule–molecule interaction energy;  $N_i$  is the number of molecular dipoles in state  $i$ ; and  $N_{ij}$  ( $i, j = \text{L, H}$ ) is the number of  $ij$  nearest-neighbor interactions. In evaluating  $\epsilon(0)$  we employ the usual relations  $N_{\text{LH}} = cN_{\text{L}} - 2N_{\text{LL}} = cN_{\text{H}} - 2N_{\text{HH}}$ , which neglect boundary effects when  $N$  is finite. The canonical partition sum of the monolayer is

$$Z' = \sum_{N_{\text{H}}=0}^N \sum_{N_{\text{LH}}} e^{-\epsilon(E)/kT} \quad (1)$$

where the second sum considers all possible values for the number of LH pairs. Taking the monolayer in the state L ( $N_{\text{L}} = N$ ) as the reference state,  $Z'_{\text{L}} = e^{(p_{\text{L}}E - \epsilon_{\text{L}}^{\circ})N/kT}$ , and using the mean-field approximation,<sup>20,21</sup>  $\epsilon(0) \approx N_{\text{L}}\epsilon_{\text{L}}^{\circ} + N_{\text{H}}\epsilon_{\text{H}}^{\circ} + (cN_{\text{H}}N_{\text{L}}/2N)\Delta\epsilon$ , the partition sum can be evaluated as

$$Z(T, N) \equiv \frac{Z'}{Z'_{\text{L}}} \approx \sum_{N_{\text{H}}=0}^N \binom{N}{N_{\text{H}}} s^{N_{\text{H}}} \sigma^{cN_{\text{H}}(1 - N_{\text{H}}/N)} \quad (2)$$

where  $s \equiv e^{(\varepsilon_L^o - \varepsilon_H^o)/kT} e^{(p_L - p_H)V/(kTd)}$  and  $\sigma \equiv e^{-\Delta\varepsilon/2kT}$ . When  $s = 1$ , the distribution of the statistical weights for the different values of  $N_H$  contributing to  $Z$  is symmetric around  $N_H = N/2$ . Therefore,  $s = 1$  corresponds to a situation where, on the average, the fraction of molecules in the state H is  $\langle x_H \rangle|_{s=1} = 1/2$ ; however, the monolayer may still have two phases of different  $\langle x_H \rangle$  at subcritical temperatures. It is then convenient to rewrite  $s = e^{(V-V_{1/2})(p_L - p_H)/(kTd)}$  where

$$V_{1/2} \equiv (\varepsilon_H^o - \varepsilon_L^o)d/(p_L - p_H) \quad (3)$$

is the switching voltage. This is the applied voltage that makes equal the energies of the two (pure) molecular states,  $\varepsilon_L^o - p_L E = \varepsilon_H^o - p_H E$  (Figures 1a and 1b). In the noncooperative case,  $\sigma = 1$  and  $Z_{NC} = (1 + s)^N$ , the average fractions of dipoles in the states L and H satisfy the relation  $s = \langle x_H \rangle / \langle x_L \rangle$ , and then  $s$  is the equilibrium constant for the  $L \rightleftharpoons H$  transition. In the cooperative case with  $\Delta\varepsilon > 4kT/c$ , the molecular interactions make the  $L \rightleftharpoons H$  molecular switching a first-order phase transition.

The average fraction of molecules in the high conductance state can be calculated as a function of the monolayer characteristics (dipole moments, interaction energies, and total number of molecules) and the external conditions (temperature and voltage) as

$$\langle x_H \rangle = \frac{1}{N} \frac{\sum_{N_H=0}^N \binom{N}{N_H} N_H s^{N_H} \sigma^{cN_H(1 - N_H/N)}}{\sum_{N_H=0}^N \binom{N}{N_H} s^{N_H} \sigma^{cN_H(1 - N_H/N)}} \quad (4)$$

which requires the numerical evaluation of the sums. The approximation of the partition sum in eq 2 by its largest term leads to the alternative expression

$$\frac{\langle x_H \rangle}{1 - \langle x_H \rangle} = s\sigma^{c(1 - 2\langle x_H \rangle)} \quad (5)$$

which resembles the Frumkin–Fowler–Guggenheim isotherm. Equations 4 and 5 clearly show that  $\langle x_H \rangle$  is a function of the variables  $s$  and  $\sigma$  that monotonously increases with  $s$ ;  $\langle x_H \rangle$  in eq 4 depends also on  $N$ . The conditions  $(\partial s / \partial \langle x_H \rangle)_\sigma = 0$  and  $(\partial^2 s / \partial^2 \langle x_H \rangle)_\sigma = 0$  allow us to determine the critical temperature from eq 5 as  $T_c = c\Delta\varepsilon/4k$ , which is the well-known mean-field result for a lattice binary system. When the  $L \rightleftharpoons H$  molecular switching is a first-order phase transition at  $T < T_c$  and  $N \rightarrow \infty$ , the binodal curve can be obtained by imposing  $s = 1$  in eq 5. Note, however, that for finite-size systems the  $L \rightleftharpoons H$  transition at  $T < T_c$  is not abrupt (it occurs over a temperature range that narrows with increasing  $N$ ), and we study it making use of eq 4.

## RESULTS AND DISCUSSION

The monolayer conductance can be estimated as<sup>11</sup>  $g = (1 - \langle x_H \rangle)g_L + \langle x_H \rangle g_H$  where  $\langle x_H \rangle$  is evaluated from eq 4 as a function of  $s = e^{(V-V_{1/2})(p_L - p_H)/(kTd)}$  and the cooperativity parameter  $\sigma = e^{-2T/cT}$ . We introduce the following system parameters  $N = 200$  (unless otherwise stated),  $c = 4$ ,  $T_c = 250$  K,  $p_L - p_H = 10$  D (1 D =  $3.3 \times 10^{-30}$  C m), and  $d = 3$  nm. The transition energy barrier<sup>5</sup>  $\varepsilon_H^o - \varepsilon_L^o = 5kT$  at 300 K corresponds to a switching voltage  $V_{1/2} \equiv (\varepsilon_H^o - \varepsilon_L^o)d/(p_L - p_H) = 1.86$  V (Figure 2a). The value of  $p_L - p_H$  has been deliberately chosen in the high range of typical dipole moments<sup>11,14,16,17</sup> to better show the concepts involved. We take  $g_H/g_L = 50$  and a typical electric field  $|E| = |V|/d \approx$

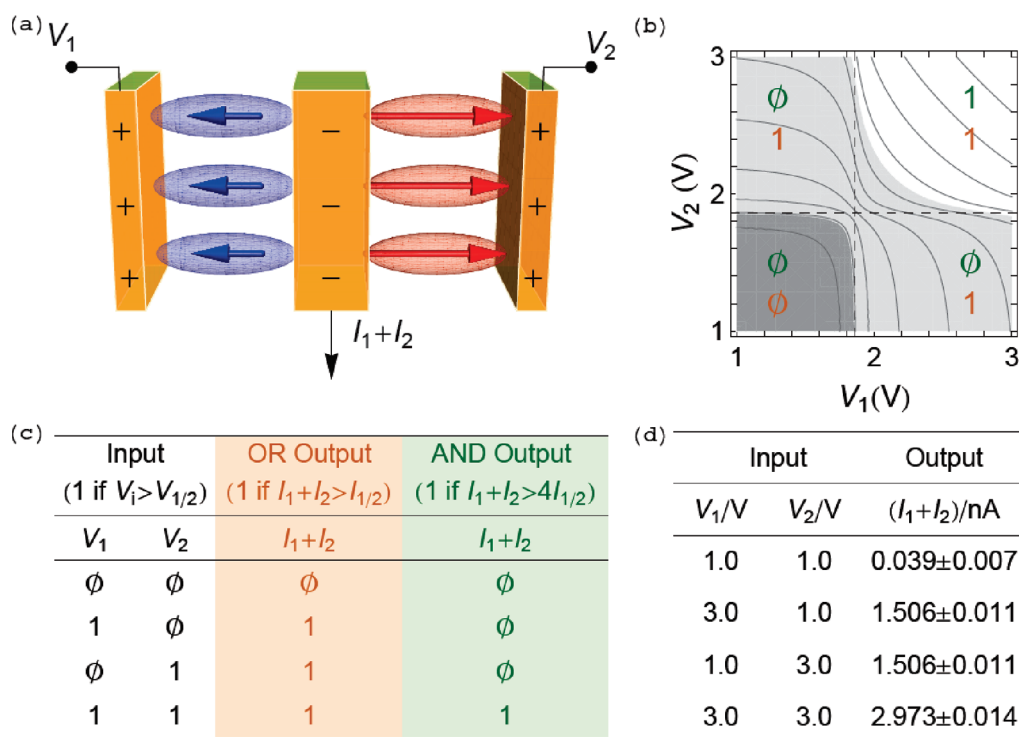
1 V/3 nm =  $3 \times 10^8$  V/m so that the electrical energy is several times the thermal energy,  $(p_L - p_H)V/(kTd) \approx 3$  for  $V = 1$  V at 300 K, which can be considered as realistic values.<sup>3,5,9–11,23</sup>

Figure 2a shows the monolayer current ( $I$ )–voltage ( $V$ ) and rectification characteristics (inset) curves parametrically in the ratio between the transition barrier and thermal energies. It reproduces qualitatively the experimental trends shown in Figure 4 of ref 1 and Figure 2 of ref 8 for the case of light-induced switching. The thermal noise, which is responsible for the broadening of the curves, has been evaluated by substituting  $\langle x_H \rangle \pm \sigma \langle x_H \rangle$  in  $g = (1 - \langle x_H \rangle)g_L + \langle x_H \rangle g_H$ , where  $\sigma \langle x_H \rangle \equiv [(\langle x_H^2 \rangle - \langle x_H \rangle^2)]^{1/2}$  has been calculated from  $Z$  in eq 2. Figure 2b shows the temperature dependence of the current–voltage curve. It can be explained from the fraction of molecules in the high conductance state of Figure 2c. The transition between the monolayer low and high conductance states occurs around  $V = V_{1/2}$  when  $T < T_c$ . Sharp transitions in the molecule isomerization with the voltage have also been observed experimentally (Figure 2 of ref 6). From the comparison with the noncooperative behavior also shown in Figure 2c we conclude that cooperativity enhances the switching response by decreasing the width of the voltage range where the transition between the high ( $g_H$ ) and low conductance ( $g_L$ ) states occurs. This voltage range can be narrowed further by increasing the dipole moment difference ( $p_L - p_H$ ) and the critical temperature. Note that it is the sharp increase in this fraction that causes the conductance switching shown in Figure 2a. Finally, the contour plot of Figure 2d shows the influence of the external parameters  $V$  and  $T$  on the monolayer state. Below the critical temperature the switching occurs as a first-order phase transition, and hence bit assignment and data storage becomes possible. Above the critical temperature the fraction of molecules in state H changes smoothly with increasing  $V$ , but the conductance change is still rather abrupt (Figure 2a) because  $g_H \gg g_L$ <sup>1,5</sup> provided that  $T/T_c$  is not so large that cooperative effects become negligible.

For realistic values of the system parameters,  $T_c = c\Delta\varepsilon/4k$  can be relatively low, but significant cooperative effects due to dipole interactions have been observed at ambient temperature for some systems.<sup>2,16,17</sup> Interestingly, the microscopic details of the local interactions are not essential provided that  $\Delta\varepsilon > 0$ . This could be the case for relatively high values of  $\varepsilon_{LH}$  due to the increased electrical and deformation energies associated with the charge and elastic mismatches that occur when molecules in states of different conformation and dipole moment coexist in the monolayer domain.<sup>14,17</sup> Note finally that approximately defined molecular architectures<sup>2,4,14,17</sup> are currently available.

One serious concern in experimental monolayers is the relatively small number of molecules forming the domain. The finite-size effects can also be analyzed with this model, as shown in Figure 2c (inset): a monolayer with only  $N = 50$  dipoles at  $T/T_c = 0.8$  shows a transition region a few tenths of volt wide, which is much narrower than that of the noncooperative case. Finite-size effects widen the transition region, but the switching becomes practically independent of  $N$  for just a few hundred dipoles.

Interestingly, because the dipole monolayer acts as an effective nanodiode (Figure 2a), the logical gates OR and AND could be implemented by exploiting the  $I$ – $V$  curves of two monolayers, as shown schematically in Figure 3a. The contour plot of Figure 3b gives the applied voltage regions where the two gates should be operative because of the electrical rectification characteristics of the monolayers (Figure 2a). The voltages applied to the two monolayers are the *inputs*, and the sum of the resulting currents  $I_1$



**Figure 3.** Scheme of the OR and AND logic gates based on two monolayers arranged back-to-back (a). The contour plot of  $I_1 + I_2$  vs  $V_1$  and  $V_2$  shows the voltage regions corresponding to the 0 and 1 outputs of the logic gates (b). The boundaries delimiting the shading (dark gray, gray, and white) regions correspond to the currents  $I_{1/2} = 0.475$  nA and  $4I_{1/2} = 1.90$  nA. The contour lines correspond to the values  $I_1 + I_2 = 0.2S, 0.50, \dots, 2.75$  nA and the dashed lines to  $V_i = V_{1/2}$ . The truth tables (c) are obtained with the monolayer potentials as the inputs and the current sum  $I_1 + I_2$  as the output (c and d). Two different current sums are used for logic output “1” in the OR and AND gates, as shown in the contour plot. The current uncertainties are estimated from the noise in the respective  $I$ – $V$  curve (Figure 2a).

$+ I_2$  is the output in the truth tables of Figure 3c and 3d. The two gates could be implemented with the same scheme by using two different threshold currents for logic output “1”:  $I_1 + I_2 > I_{1/2}$  in the case of the OR gate and  $I_1 + I_2 > 4I_{1/2}$  in the case of the AND gate, where  $I_{1/2} = (g_H + g_L)V_{1/2}/2$  is the current across a monolayer in a state with  $\langle x_H \rangle = 1/2$ . We have used  $\epsilon_H^0 - \epsilon_L^0 = 5kT$ ,  $T = 300$  K, and  $g_H = 50g_L = 500$  pS in Figure 3b and 3d, so that  $V_{1/2} = 1.86$  V and the boundaries delimiting the shading regions (dark gray for outputs “0” of the OR gate and “0” of the AND gate, gray for outputs “1” of the OR gate and “0” of the AND gate, and white for outputs “1” of the OR gate and “1” of the AND gate) correspond to the output currents  $I_{1/2} = 0.475$  nA and  $4I_{1/2} = 1.90$  nA.

Because molecular dipoles are characteristic of biophysical structures, the results are also relevant for biological membranes and biosensors.<sup>20–22</sup> In particular, the dipole monolayer could be used as the active layer for a sensor immersed in a solution of a ligand that binds to the molecular dipoles.<sup>16,22</sup> If the ligand binds preferably to the dipoles in one particular state, the ligand concentration (in addition to the applied voltage) modulates the monolayer conductance because it shifts the  $L \rightleftharpoons H$  equilibrium. Assuming that the ligand binds only to the dipoles in the H state, the grand canonical partition function of a monolayer in contact with a solution of ligand molar concentration  $c_1$  is<sup>12,20,21</sup>

$$\Xi(T, N, c_1) = \sum_{N_H=0}^N \binom{N}{N_H} s^{N_H} (1 + Kc_1)^{N_H} \sigma^{cN_H(1 - N_H/N)} \quad (6)$$

where  $K$  is the equilibrium binding constant for the ligand. The product<sup>26</sup>  $Kc_1$  is equal to  $\lambda_1 z_1$  where  $\lambda_1 \equiv e^{\mu_1/kT}$  is the absolute

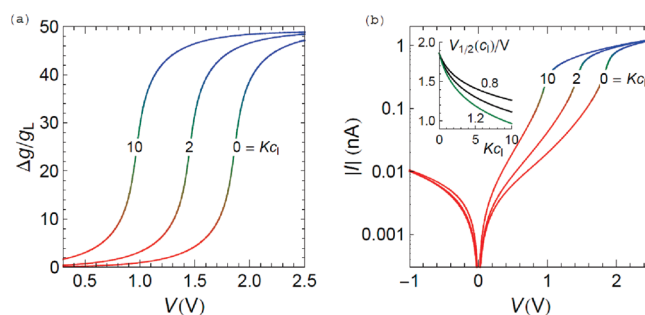


**Figure 4.** Relative conductance change  $\Delta g/g_L$  vs  $V$  (a) and the  $I$ – $V$  curves in logarithmic scale (b) for  $T = 300$  K,  $(\epsilon_H^0 - \epsilon_L^0)/k = 1500$  K,  $g_L = 10$  pS, and different ligand concentrations given by  $Kc_1$ . The curves have been colored according to the  $\langle x_H \rangle$  values as shown in Figure 2d. The inset shows the switching voltage  $V_{1/2}(c_1)$  vs  $Kc_1$  for  $(\epsilon_H^0 - \epsilon_L^0)/k = 1500$  K and the temperature ratios  $T/T_c = 0.8, 1.0, 1.2$  (b); the green curve in the inset corresponds to  $T/T_c = 1.2$  and  $T = 300$  K.

activity of the ligand (which is proportional to  $c_1$  in a dilute solution);  $\mu_1$  is the ligand chemical potential; and  $z_1$  is the canonical partition function of the ligand bound to a molecular dipole in state H. From eq 6, the average fraction of dipoles in state H is given by eq 4 (or eq 5) with  $s$  replaced by  $s(c_1) \equiv s(1 + Kc_1)$ . Therefore, the presence of the ligand favors the molecular state H. Moreover, since  $\langle x_H \rangle = 1/2$  corresponds to  $s(c_1) = 1$ , the switching potential depends on the ligand concentration as  $V_{1/2}(c_1) = V_{1/2}(0) - [dkT/(p_L - p_H)] \ln(1 + Kc_1)$ , where the value  $V_{1/2}(0)$  corresponds to the zero ligand concentration (eq 3).

Figure 4a for the relative conductance increase  $\Delta g/g_L = 49\langle x_{\text{H}} \rangle$  shows that the presence of the ligand shifts the  $L \rightleftharpoons H$  equilibrium favoring the molecular state H:  $\langle x_{\text{H}} \rangle$  and the monolayer conductance at a given voltage  $V$  increase with the ligand concentration. The resulting decrease in the switching potential is shown in the inset of Figure 4b. This figure demonstrates also that the monolayer rectification characteristics can be modulated by  $K_{\text{Cl}}$ : the ligand concentration is responsible for the gating of the monolayer, which acts then as an effective *chemical transistor*. Note that the active layer where the ligand binding occurs could also give a potentiometric signal (as opposed to the conductance-based output of Figure 4). Indeed, the dipolar changes in the monolayer should also produce measurable electric potential changes<sup>22</sup> because the binding of the ligands to the molecular dipoles occurs with local charge redistribution or transfer.<sup>16,17</sup>

## CONCLUSION

Addressing a small domain of molecules anchored at a surface not only avoids the need for accessing single molecules in a reproducible manner<sup>27,28</sup> but also offers the possibility of using the emerging cooperative properties in the design of switches robust against the finite-size effects inherent to the nanoscale. As a proof-of-concept, we show that the local interactions between adjacent molecules in a densely packed monolayer can stabilize domains of molecules predominantly in the same molecular state enhancing field-induced conductance switching. This result should be useful for bit assignment and data storage modes, the implementation of logic gates, and the design of a sensing layer. We note finally that small reshapes of the molecular electron densities in the monolayer rather than conductances could also be used as the output because of the cooperative action of many molecules acting together to give an enhanced electrical signal. These changes in the local electron density should correlate with the average fractions of dipoles in the different states.

## AUTHOR INFORMATION

### Corresponding Author

\*E-mail: smafe@uv.es.

## ACKNOWLEDGMENT

Financial support from the Ministry of Science and Innovation of Spain (project MAT2009-07747) and FEDER is acknowledged.

## REFERENCES

- (1) Smaali, K.; Lenfant, S.; Karpe, S.; Ocafrain; Blanchard, M. P.; Deresmes, D.; Godey, S.; Rochefort, A.; Roncali, J.; Vuillaume, D. *ACS Nano* **2010**, *4*, 2411–2421.
- (2) Pace, G.; Ferri, V.; Grave, C.; Elbing, M.; von Hänisch, C.; Zharnikov, M.; Mayor, M.; Rampi, M. A.; Samor, P. *Proc. Natl. Acad. Sci.* **2007**, *104*, 9937–9942.
- (3) Guo, W.; Du, S. X.; Zhang, Y. Y.; Hofer, W. A.; Seidel, C.; Chi, L. F.; Fuchs, H.; Gao, H.-J. *Surf. Sci.* **2009**, *603*, 2815–2819.
- (4) Alemani, M.; Peters, M. V.; Hecht, S.; Reider, K.-H.; Moresco, F.; Grill, L. *J. Am. Chem. Soc.* **2006**, *128*, 14446–14447.
- (5) Yasuda, S.; Nakamura, T.; Matsumoto, M.; Shigekawa, H. *J. Am. Chem. Soc.* **2003**, *125*, 16430–16433.
- (6) Henzl, J.; Melhorn, M.; Gawronski, H.; Reider, K.-H.; Morgenstern, K. *Angew. Chem., Int. Ed.* **2006**, *45*, 603–606.

- (7) Russev, M.-M.; Hecht, S. *Adv. Mater.* **2010**, *22*, 3348–3360.
- (8) Ferri, V.; Elbing, M.; Pace, G.; Dickey, M. D.; Zharnikov, M.; Samori, P.; Mayor, M.; Rampi, M. A. *Angew. Chem., Int. Ed.* **2008**, *47*, 3407–3409.
- (9) Fuchs, G.; Klamroth, T.; Dokic, J.; Saalfrank, P. *J. Phys. Chem. B* **2006**, *110*, 16337–16345.
- (10) Chapman, C.; Paci, I. *J. Phys. Chem. C* **2010**, *114*, 20556–20563.
- (11) Troisi, A.; Ratner, M. A. *J. Am. Chem. Soc.* **2002**, *124*, 14528–14529.
- (12) Hill, T. L. *Proc. Natl. Acad. Sci.* **1967**, *58*, 111–114.
- (13) Feldheim, D. L.; Keating, C. D. *Chem. Soc. Rev.* **1998**, *27*, 1–12.
- (14) Kimura, S. *Org. Biomol. Chem.* **2008**, *6*, 1143–1148.
- (15) Cervera, J.; Manzanares, J. A.; Mafé, S. *Nanotechnology* **2009**, *20*, 465202.
- (16) Cahen, D.; Naaman, R.; Vager, Z. *Adv. Funct. Mater.* **2005**, *15*, 1571–1578.
- (17) Sfez, R.; Peor, N.; Yitzchaik, S. *J. Phys. Chem. C* **2010**, *114*, 20531–20538.
- (18) Yaliraki, N.; Longo, G.; Gale, E.; Szleifer, I.; Ratner, M. A. *J. Chem. Phys.* **2006**, *125*, 074708.
- (19) Chapman, C. R. L.; Paci, I. *J. Phys. Chem. C* **2010**, *114*, 2645–2654.
- (20) Hill, T. L. *Cooperativity Theory in Biochemistry: Steady-state and Equilibrium Systems*; Springer: Berlin, 1985.
- (21) Ben-Naim, A. *Cooperativity and Regulation in Biochemical Processes*; Plenum: New York, 2000.
- (22) Goykhman, I.; Korbakov, N.; Bartic, C.; Borghs, G.; Spira, M. E.; Shappir, J.; Yitzchaik, S. *J. Am. Chem. Soc.* **2009**, *131*, 4788–4794.
- (23) Das, B.; Abe, S. *J. Phys. Chem. B* **2006**, *110*, 4247–4255.
- (24) Lewis, P. A.; Inman, C. E.; Maya, F.; Tour, J. M.; Hutchison, J. E.; Weiss, P. S. *J. Am. Chem. Soc.* **2005**, *127*, 17421–17426.
- (25) Blum, A. S.; Kushmerick, J. G.; Long, D. P.; Patterson, C. H.; Yang, J. C.; Henderson, J. C.; Yao, Y.; Tour, J. M.; Shashidhar, R.; Ratna, B. R. *Nat. Mater.* **2005**, *4*, 167–172.
- (26) Mafé, S.; Garcia-Morales, V.; Ramírez, P. *Chem. Phys.* **2004**, *296*, 29–35.
- (27) Cervera, J.; Mafé, S. *ChemPhysChem* **2010**, *11*, 1654–1659.
- (28) Szacilowski, K. *Chem. Rev.* **2008**, *108*, 3481–3548.